

Alma Mater Studiorum Università di Bologna
Archivio istituzionale della ricerca

Surface charging on HVDC spacers considering time-varying effect of temperature and electric fields

This is the final peer-reviewed author's accepted manuscript (postprint) of the following publication:

Published Version:

Yan, W.u., Li, C., Lei, Z., Han, T., Zhang, Z., Fabiani, D. (2019). Surface charging on HVDC spacers considering time-varying effect of temperature and electric fields. IEEE TRANSACTIONS ON DIELECTRICS AND ELECTRICAL INSULATION, 26(4), 1316-1324 [10.1109/TDEI.2019.008021].

Availability:

This version is available at: <https://hdl.handle.net/11585/744287> since: 2020-03-02

Published:

DOI: <http://doi.org/10.1109/TDEI.2019.008021>

Terms of use:

Some rights reserved. The terms and conditions for the reuse of this version of the manuscript are specified in the publishing policy. For all terms of use and more information see the publisher's website.

This item was downloaded from IRIS Università di Bologna (<https://cris.unibo.it/>).
When citing, please refer to the published version.

(Article begins on next page)

This is the final peer-reviewed accepted manuscript of:

W. Yan, C. Li, Z. Lei, T. Han, Z. Zhang and D. Fabiani, Surface charging on HVDC spacers considering time-varying effect of temperature and electric fields

in IEEE Transactions on Dielectrics and Electrical Insulation, vol. 26, no. 4, pp. 1316-1324, Aug. 2019

The final published version is available online at:

<https://doi.org/10.1109/TDEI.2019.008021>

Rights / License:

The terms and conditions for the reuse of this version of the manuscript are specified in the publishing policy. For all terms of use and more information see the publisher's website.

This item was downloaded from IRIS Università di Bologna (<https://cris.unibo.it/>)

When citing, please refer to the published version.

Surface Charging on HVDC Spacers Considering Time-varying Effect of Temperature and Electric Fields

Wu Yan

School of Electrical Engineering, Shanghai University of Electric Power
Changyang Road #2588, Shanghai, 200090, China

Chuanyang Li

Department of Electrical, Electronic, and Information Engineering “Guglielmo Marconi”, University of Bologna, Viale
Risorgimento 2, Bologna, 40136, Italy

Zhipeng Lei

Shanxi Key Laboratory of Mining Electrical Equipment and Intelligent Control, College of Electrical and Power
Engineering, Taiyuan University of Technology, Taiyuan, 030024, China

Tao Han

Key Laboratory of Smart Grid of Education Ministry, School of Electrical and Information Engineering
Tianjin University, Tianjin 300072, China

Zhousheng Zhang

School of Electrical Engineering, Shanghai University of Electric Power
Changyang Road #2588, Shanghai, 200090, China

Davide Fabiani

Department of Electrical, Electronic, and Information Engineering “Guglielmo Marconi”, University of Bologna, Viale
Risorgimento 2, Bologna, 40136, Italy

ABSTRACT

The dynamic behavior of surface charging on spacers in DC-GILs can be influenced by multi-factors including the non-uniform distributed electric field as well as the time-varying temperature gradient. In this paper, the time-varying effect of surface charging phenomenon on spacers is studied and a time-varying mathematical model is established, based on the influence of temperature and electric field on the ion mobility at the gas phase and the bulk conductivity in the solid phase. The results verify that the bulk conductivity can be greatly influenced by temperature, which leads to an increase in the surface charge density on the spacer. This allows the surface charge accumulation to stabilize more quickly. However, the ion mobility from the gas phase is less affected by temperature. When the non-uniform distributed electric field changes from 1.3 to 6.4 kV/mm, ion mobility is less influenced and the surface charge density on the spacer varies slightly. In this case, the effects of the non-uniformly distributed electric field in surface charge density variation is much smaller and can be ignored.

Index Terms — HVDC, GIL, spacer, surface charge accumulation, temperature, electric field

1 INTRODUCTION

WITH the unbalanced distribution of energy resources and electric loading increment, technologies for large-scale energy storage and long-distance transmission are becoming increasingly important. Gas-insulated power transmission lines (GILs) which have advantages of large capacity with a

compact and flexible arrangement and high stability, can provide a superior choice to replace overhead transmission lines in certain environments [1]. However, restricted by surface charging of spacers under DC field, there are still reports about the industry application of DC-GILs. Surface charge accumulation can distort the electric field on the spacer surface, which may reduce the surface flashover

voltage and thus decrease the robustness of the electric power transmission system [2].

Researches regarding charge dynamics in HVDC GIS/GIL have been performed for several decades [3-5]. It is generally thought that surface charge on GIL spacers originate from three sources [6]: (1) conduction through the volume; (2) conduction within the gas phase; and (3) conduction along the spacer surface. However, due to the complexity of the surface charge behavior and the uncontrollable external interference during surface charge measurement, studies by means of simulation provides favorable assistance for uncovering this crack problem in recent years.

According to European researchers, the temperature gradient due to conduction of DC current led to uneven variation in solid bulk conductivity, which can affect the accumulation property of space charge and distort the electric field over the spacers [7, 8]. He *et al* [9] studied the thermal gradient effected on surface charge. The results show that the expansion of an analogous ineffective region near HV electrode results in a large voltage drop across the area near the ground electrode. Under these conditions, positive streamers can be triggered at the triple junction of the ground electrode more easily [9]. Ma suggested that the conduction through the volume dominates the surface charge accumulation in DC-GILs; the space charge density of the spacer increases significantly with increased temperature of the center electrode [5, 10].

In most previous studies, the conductivity and ion mobility have been set as a constant value. However, in practice, the conductivity of spacers and the ion mobility in the insulating gas are influenced by many factors, such as temperature variation and field strength distribution [11,12]. The temperature distribution variation of the spacer and the non-uniform distributed electric field strength can influence the surface charging behavior, which in turn, can affect the distribution of the electric field stresses, resulting a mutual influence effect. Therefore, it is necessary to consider the effects of temperature distribution variation and the non-uniform distributed electric field strength on surface charge dynamic process during simulations.

In this paper, a time-varying mathematical model is established, based on the influence of temperature and electric field strength on ion mobility at the gas phase and the bulk conductivity in the solid phase. The relationships between gas ion mobility and solid conductivity was discussed. The effects of temperature and electric field intensity on surface charge variation was investigated. The mechanism of charge dynamics affected by temperature and electric field intensity on a disc-type spacer inside a DC-GIL was concluded.

2 PARAMETER SETTINGS AND BOUNDARY CONDITIONS

The accumulation and decay of surface charges on the disc spacer in a DC-GIL is affected by electric conduction via the bulk volume, conduction within the gas phase, and conduction along the spacer surface. This is a dynamic, instantaneous process that continues until the accumulation and dissipation reach a dynamic equilibrium. However, the

electric conduction along the spacer surface is generally considered to play a minor role in surface charge accumulation, unless the surface has been modified to have a higher conductivity [13]. Therefore, the mathematical model in this paper does not take it into account surface conduction.

Figure 1 shows the representation of normal vectors on the spacer surface. As a result, the spacer gas-solid interface can be described by the following equation:

(1)

where n_b is the normal component on the spacer solid-side of the interface, n_g is the normal component on the spacer gas-side of the interface; j_b is the current density on the spacer solid-side of the interface, j_g is the current density on the spacer gas-side of the interface, ρ^* is the surface charge density, .

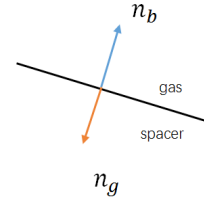


Figure 1. Representation of normal vectors on the spacer surface.

2.1 CONDUCTION IN GAS PHASE

Assuming that the dielectric constant of the insulating gas is not affected by the temperature and the electric field strength, the relationship between the positive charge density ρ^+ , the negative charge density ρ^- , and the potential can be expressed by Poisson's equation:

(2)

Considering the generation, recombination, migration, and diffusion processes of ions in DC GIL, the current continuity equation can be written as:

(3)

where J is the current density, R is the recombination coefficient, e is the elementary charge, n_0 is the ionization rate, .

The current densities are given by:

(4)

where μ^\pm are the corresponding ion mobilities, D is the diffusion coefficient, .

Because the ion mobility dominates in the insulating gas, the ion diffusion rate is neglected [7]. Finally, inserting Equation (4) into Equation (3) results in:

(5)

Equations (2) and (5) determine the ion flow field within the gaseous medium.

2.2 CHARGING IN VOLUME

In the volume domain (referred to the bulk in the following content), the spacer charge density ρ and the potential ϕ are connected via:

(6)

while the equation of continuity is:

(7)

The current density is given by the conductivity σ , which is assumed to be independent of the electric field by the following equation:

(8)

Taking the time derivative of (6) and inserting (7) and (8) results in:

Equation (9) determines the charging of the bulk. (9)

2.3 PARAMETERS OF TEMPERATURE DISTRIBUTION MODEL

The surface conductivity of the disc spacer changes with temperature variation, which can affect the surface charge accumulation and decay process of the disc spacer in the DC-GIL. At the same time, the degree of kinetic motion of the particles in the gas changes with temperature, and these changes in the kinetic energy of the particles also lead to changes in the ion mobility.

The main heat transfer mechanisms in the DC-GIL are solid heat transfer and fluid heat transfer. The solid heat transfer mainly occurs via heat conduction, and the fluid heat transfer mainly via heat convection, according to Fourier's law [14]:

$$(10)$$

$$(11)$$

where ρ is the density of the object, kg/m^3 ; C is the specific heat capacity of the object, $J/(kg \cdot K)$; T is the temperature, K ; k is the thermal conductivity of the object, $W/(m \cdot K)$; t is the velocity field of the fluid, s ; q is the heat flux of the object, W/m^2 ; Q is the heat sources, W/m^3 .

The typical temperature of the center conductor and the grounded enclosure of the DC-GIL during rated operation are T_c , T_g [7], and the spacer is in direct contact with the insulating gas. The thermal properties of the two phase cause coupling heat transfer on the surface of the spacer. The heat flux and temperature at the gas-solid interface in the model of DC-GIL conjugate heat transfer are equaled by:

$$(12)$$

$$(13)$$

where T_{spoxy} , T_{SF6} are the temperature of the spacer and the insulating gas at the gas-solid interface, K ; q_{spoxy} , q_{SF6} are the heat flux of the spacer and the insulating gas at the gas-solid interface, W/m^2 .

The solid conductivity and gas ion mobility are not constant due to the temperature variation. Therefore, the relationship between the solid electrical conductivity and the temperature of the disc spacer can be expressed by an empirical formula [8]:

$$(14)$$

where σ_g is the conductivity at initial temperature and electric field strength, ; α is the temperature coefficient of conductivity, .

The relationship between the positive or negative ion mobility and temperature in the insulating gas is as follows [12]:

$$(15)$$

where μ_0^{\pm} is the initial positive or negative ion mobility, ; P_0 is the reference pressure, ; T_0 is the reference temperature, .

2.4 PARAMETERS OF ELECTRIC FIELD MODEL

During operation, the distribution of the electric field strength in the DC-GIL during operation are not uniform parameters, due to temperature changing. Also, the electric field strength in the spacer of DC GIL is relatively large, i.e. on the order of magnitude up to 1 MV/m [8]. The conductivity of the spacer should be as a consequence higher than that when no voltage was applied. The changing of

electric field strength can affect the amount of energy obtained by the ions from the electric field and thus influence the ion mobility [12]. Therefore, for the disc spacer, the conductivity varies among different positions, and the ion mobility of the insulating gas is also position-dependent.

The relationship between the positive charge density ρ^+ , the negative charge density ρ^- , and the potential ϕ in the DC-GIL can be expressed by the Poisson Equation (2). The relationship between the electric field strength E and the potential ϕ can be expressed by Laplace's equation:

$$(16)$$

The mobility of the positive or negative ions in the SF_6 gas varies with E . This variation can be obtained by the relationship between the mobility at high field strength and the electric field strength E by the following equation [12]:

$$(17)$$

where A , B are material coefficients, .

The relationship between solid conductivity and the field strength of the disc spacer can be expressed by an empirical formula [8]:

$$(18)$$

where β is the conductivity coefficient of the field strength, mm/kV .

2.5 BOUNDARY CONDITIONS OF DC GIL SIMULATION MODEL

Figure 2. Boundary condition of DC GIL simulation model (Unit: mm).

Based on the typical 220 kV AC GIL size in actual operations [15], the simulation model of the GIL is established using COMSOL, as shown in Figure 2. In this model, the center conductor length (adjacent to the gas) is 450 mm; the radii of the center conductor are 50 mm and 20.75 mm, respectively; the distance from the center conductor to the inner side of the ground enclosure is 206.25 mm; the thicknesses of the spacer near the center conductor and near the ground enclosure are 50 and 25 mm, respectively. It should be noted that the GIL model is displayed vertically for convenience in dimensioning.

During the simulation of surface charge accumulation, it is assumed that the DC-GIL is operating indoors, where the environment is dry and the temperature is constant inside the DC-GIL.

The boundary conditions are as follows: center conductor voltage , grounded enclosure .

The positive ion density at the side boundary of the junction between insulating gas and center conductor is bounded by the Dirichlet condition, and the negative ion density at the surface of the disc spacer is bounded by the Neumann condition:

$$(19)$$

Likewise, the negative ion density at the side boundary of the interface between insulating gas and ground enclosure is bounded by the Dirichlet condition, and the positive ion density at the surface of the disc spacer is bounded by the Neumann condition:

$$(20)$$

The simulation model parameters are shown in Table 1.

Table 1. Simulation model parameters.

Parameter	Physical quantity	Value	Reference
	positive/negative ion mobility		[7]
	recombination ion pair		[7]
	generation rate induced by natural radiation elementary charge		[7]
	Boltzmann constant		[3]
	spacer dielectric constant		[3]
	dielectric constant		[3]
	spacer solid conductivity		[3]
	initial positive/negative ion density		[3]
	spacer density		[14]
	density		[14]
	spacer thermal conductivity		[14]
	thermal conductivity		[14]
	spacer specific heat capacity		[14]
	specific heat capacity		[14]
	simulation pressure		[3,13]
	reference pressure		[12]
	conductivity temperature coefficient		[8]
	conductivity field strength		[8]
	coefficient reference temperature		[7]
	center conductor temperature		[7]
	wall temperature material		[7]
	coefficient material		[12]
	coefficient material		[12]

3 TIME-VARYING CHARACTERISTICS OF SURFACE CHARGE ACCUMULATION

When the ion mobility and the volume conductivity are constants (Table 1), the normal component of the electric field strengths of both surfaces of the spacer in a +400 kV GIL are shown in Figure 3 and Figure 4.

It can be seen from Figure 3 that the electric field strength on the surface of the spacer is distorted. There are two reasons. One is the streamlines of the field from the tapered shape of the inner conductor, and the other is that the electric field distribution changes with the surface charge distribution of spacer. Because of this, the electric field strength near the inner conductor is the highest at 25 mm, which is due to the most charges accumulated on the spacer surface and the SF₆ gas space nearby. On the upper side of the spacer, there are charges very near to the inner conductor as well as charges of the same polarity near to the outer conductor. These originate from the conical shape of the spacer itself. Moreover, the electric field strength close to the enclosure is lowered at first, followed by a rapidly increase. This is

due to the conical shape of the spacer.

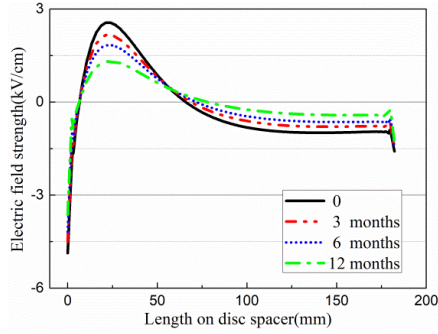


Figure 3. Normal component of the electric field on the upper spacer boundary at +400 kV.

From Figure 3 the maximum values of the normal component of the electric field strength of the upper surface of the spacer at the initial time $t = 0$, 3 months, 6 months, and 12 months are -4.87, -4.5, -4.17, and -3.63 kV/cm, respectively. These values are taken from the three-point junction (solid spacer-gas-HV electrode). As time goes on, the normal component of the electric field strength becomes smaller and smaller, the reason is the normal component of the electric field strength on the surface of the spacer is negative, positive ions on the insulating gas side drift toward the surface of the spacer, causing positive charges to accumulate over time, and the accumulated positive charges continuously weaken the solid-side normal component of the electric field strength. For the same reason, the accumulation of negative ions results in the decrease of electric field strength at 25 mm with time.

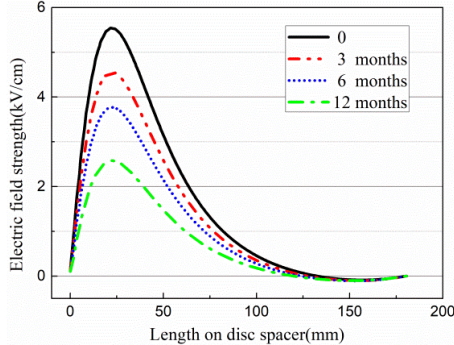


Figure 4. Normal component of the electric field on the lower spacer boundary at +400 kV.

From Figure 4 the maximum values of the normal component of the electric field strength of the lower surface of the spacer at the initial time $t = 0$, 3, 6 and 12 months are 5.55, 4.56, 3.78 and 2.58 kV/cm, respectively. There is no conical shape on the lower surface of spacer, so there is only one type of charge accumulated on the lower surface, so there is no charge moving along the surface, and the steady state (charge distribution does not change with time) is faster [16]. Therefore, the maximum normal component of the electric field strength on the lower surface decreases faster than that on the upper surface.

From Figure 5, a large part of the upper surface of the spacer accumulates positive charge, and negative charges accumulate only on a small part of the spacer's surface near the internal conductor. The reason is that the direction of the electric field line on the upper surface of the spacer mainly points from the gas side to the solid side, positive ions on the

insulating gas side drift toward the surface of the spacer, causing positive charges to accumulate over time. The maximum values for different times along the spacer surface are 0, 3.6, 6.85, and 12.95, respectively. And the charge density value increases with time. Moreover, because of the conical structure of spacer, the surface charge density close to the enclosure is greatly higher than that nearby.

From Figure 6, considerable negative charge accumulates in most areas of the lower surface of the spacer, but a small amount of positive charge accumulates on the spacer surface near the ground enclosure. The maximum values for different times along the spacer surface are 0, -3.8, -6.82, and -11.48, respectively. And the charge density value increases with time.

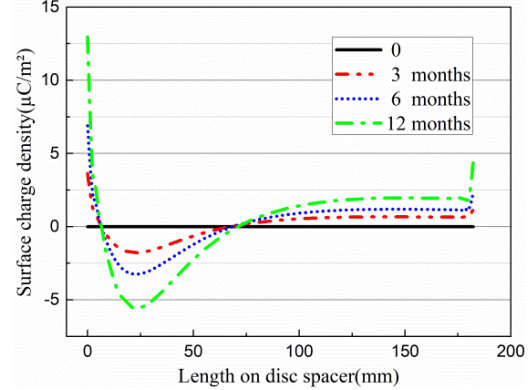


Figure 5. Surface charge density on the upper spacer boundary at +400 kV.

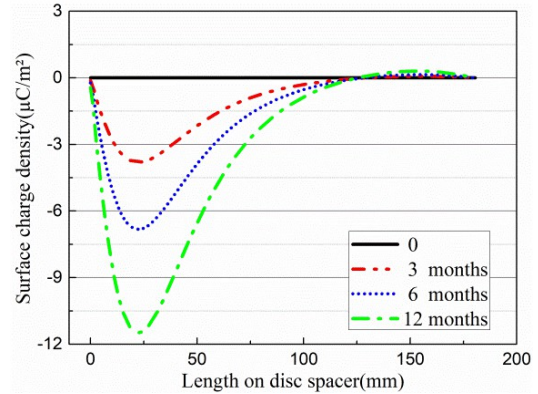


Figure 6. Surface charge density on the lower spacer boundary at +400 kV.

4 EFFECTS OF TEMPERATURE DISTRIBUTION ON SURFACE CHARGING

4.1 TEMPERATURE DISTRIBUTION IN GIL

The two-dimensional distribution map of the DC GIL temperature is shown in Figure 7. The temperature field application condition considers solid heat conduction and fluid heat convection, where the high voltage conductor temperature is 341, the ground electrode temperature is 313 K. The time when the chamber temperature is stable is 18 hours.

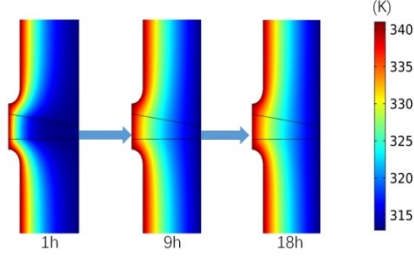


Figure 7. DC-GIL temperature distribution.

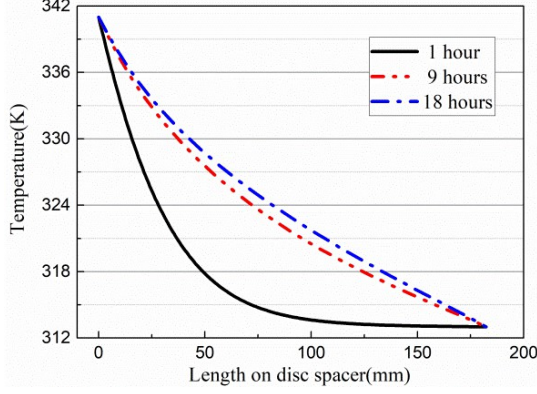


Figure 8. Temperature distribution on the upper spacer boundary.

From the time-varying curves of the temperature at various positions on the upper and lower surfaces of the spacer in Figure 8 and 9, it can be seen that the surface temperature of the DC-GIL spacer is unevenly distributed. From $t = 0$ to the steady state, the temperature distribution develops from extremely uneven to uniform. Therefore, the continually changing temperature distribution on the surface of the spacer will affect the dynamic process of surface charge accumulation and dissipation. Previous studies have failed to reflect the real dynamic state of charge accumulation on the surface of the GIL spacer because they assume a constant temperature.

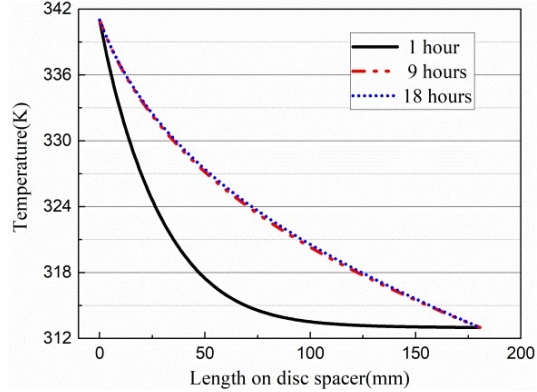


Figure 9. Temperature distribution on the lower spacer boundary.

4.2 SURFACE CHARGING MODEL UNDER TEMPERATURE DISTRIBUTION

The temperature distribution and its time-variation affect gas ion mobility and solid conductivity, which in turn affects the surface charge accumulation. The charge densities of the upper and lower surfaces of the spacer when considering the temperature change are shown in Figure 10 and 11. Therein, represents the ion mobility as a function of the changing spacer surface temperature; represents the solid conductivity as a function of the changing spacer surface temperature.

When the effects of temperature and electric field on solid conductivity and gas ion mobility are not considered, the surface charge densities at the three-point junction on the upper surface of the spacer in Figure 5 are 6.85 and 12.95, respectively, at 6 months and 1 year.

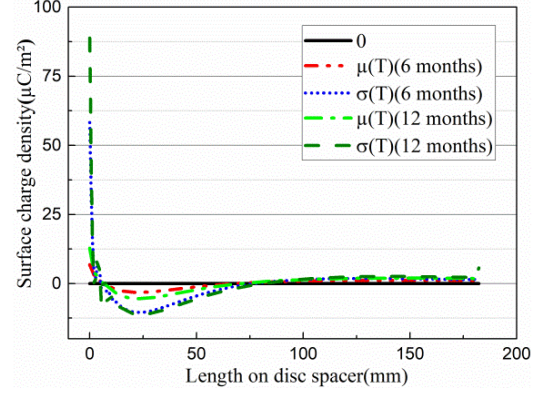


Figure 10. Surface charge density on the upper spacer boundary at +400 kV.

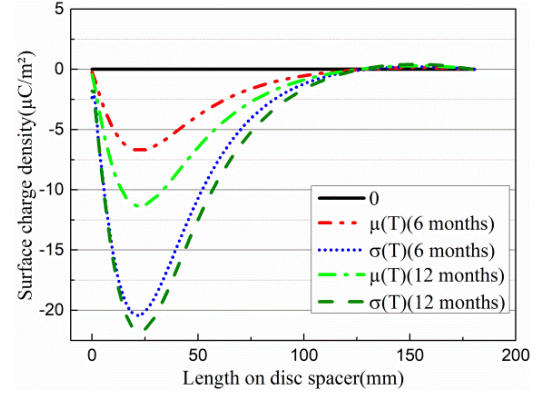


Figure 11. Surface charge density on the lower spacer boundary at +400 kV.

When considering the influence of temperature on solid conductivity, the surface charge densities at the three-point junction of the upper surface in Figure 10 at 6 months and 1 year are 58.3 and 88.5, respectively, which are respectively increased by 7.51 and 5.85 times relative to the case where temperature is neglected. From 6 months to 1 year, the growth rate of the surface charge density drops from 89 % to 51.8 %. It can be seen that when the effect of temperature is taken into account, the surface charge density of the spacers increases more sharply, and surface charge accumulation reaches a steady state more quickly. The reason is the higher the temperature, the higher the gas ion mobility and solid conductivity.

When considering the effect of temperature on the ion mobility, the surface charge densities at the three-point bond surface of the spacer at 6 months and 1 year in Figure 10 are 6.82 and 12.79. These values differ little from the case in which the influence of temperature is not considered. The ion mobility is relatively temperature-independent because the change in the surface temperature distribution of the spacer only affects the gas-side ion mobility near the surface of the spacer. These gas ions, which will soon reach or have already reached the surface, have less effect on the surface charge density.

The difference of $\sigma(t)$ between 6 months and 12 months

is much smaller than that of $\mu(t)$, the reason is the effect of temperature on solid conductivity is greater than ion mobility (see Equations (14) and (15)).

5 EFFECTS OF NONLINEAR ELECTRIC FIELD ON SURFACE CHARGING

5.1 ELECTRIC FIELD DISTRIBUTION IN GIL

The electric field strength distribution of the DC GIL model at +400 kV is simulated by COMSOL. The two-dimensional distribution map of DC GIL electric field strength is shown in Figure 12. It can be seen that the electric field strength distribution is uneven in the whole GIL cavity.

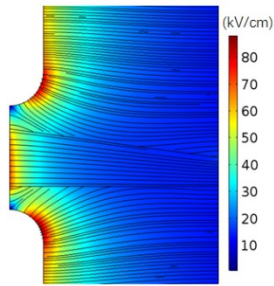


Figure 12. Simulation of synthetic electric field of DC-GIL model at +400 kV.

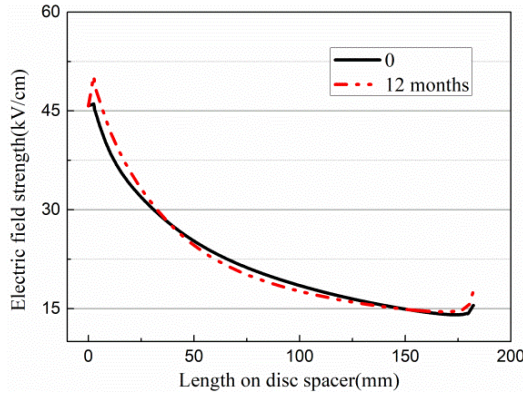


Figure 13. Synthetic electric field of the upper spacer boundary at +400 kV.

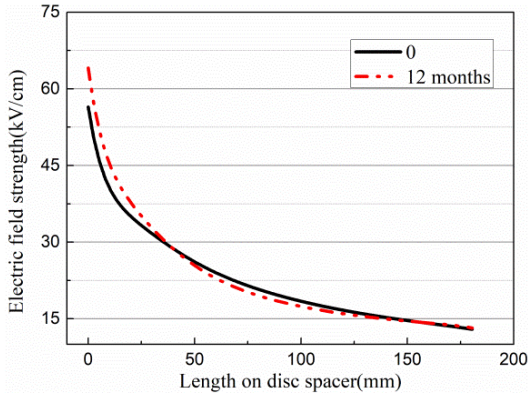


Figure 14. Synthetic electric field of the lower spacer boundary at +400 kV.

The time-varying curve distribution of the electric field strength at different positions on the upper and lower surfaces of the spacer is shown in Figure 13 and 14. It can be seen that the electric field intensity distribution on the spacer surface in the DC-GIL is not uniform, and the

distribution does not substantially change with time.

5.2 SURFACE CHARGING MODEL UNDER ELECTRIC FIELD DISTRIBUTION

The electric field strength distribution on the surface of the disc spacer affects the gas ion mobility and solid conductivity, which in turn affects the accumulation and dissipation of the surface charge and ultimately affects the surface charge distribution of the spacer. The charge densities of the upper and lower surfaces of the spacer when considering the change of field strength are shown in Figure 15 and Figure 16, confirming that both the mobility and the solid conductivity change with the electric field strength. The gas ionic mobility and the solid conductivity are no longer a fixed value, but change dynamically with the change of normal and tangential synthetic electric field strength. The synthetic electric field strength ranges from 1.3 kv/mm to 6.4 kv/mm during transient to steady state.

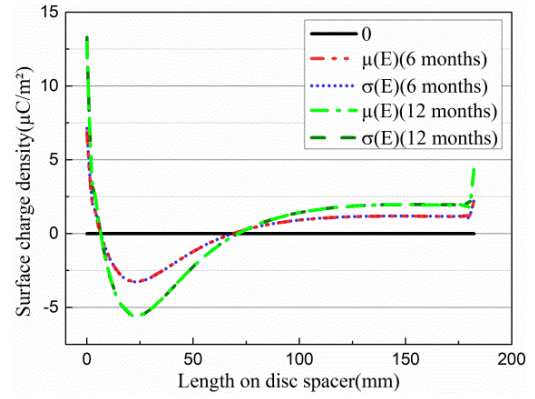


Figure 15. Surface charge density on the upper spacer boundary at +400 kV.

When considering the influence of field strength on the solid conductivity, as shown in Figure 15, the three-point junctions on the top surface of the spacers have charge densities of 7.13 and 13.3 at 6 months and 12 months, respectively. Compared with the case in which the influence of field strength is neglected, these charge densities are increased by 4.08 and 2.7%, respectively. From 6 to 12 months, the growth rate of the surface charge density decreases from 89 to 86.5%. Therefore, when considering the influence of the field strength, the surface charge density of the spacer slightly increases, and the charge accumulation rate becomes slightly faster. According to formula (18), the value of conductivity coefficient is smaller, which makes the solid conductivity less affected by electric field strength, and the increase is small, so the surface charge density and accumulation rate increase little.

When considering the influence of field strength on ion mobility, as shown in Figure 16, the surface charge densities at the three-point junction of the upper surface at 6 months and 1 year are -6.853 and -12.954, respectively, which is a little higher than those without considering the field strength. In the mathematical model of the relation between the ion mobility and the electric field intensity, the material coefficient is extremely small. Therefore, the surface charge density of the spacer changes only minimally even when considering the influence of the field strength on the ion mobility.

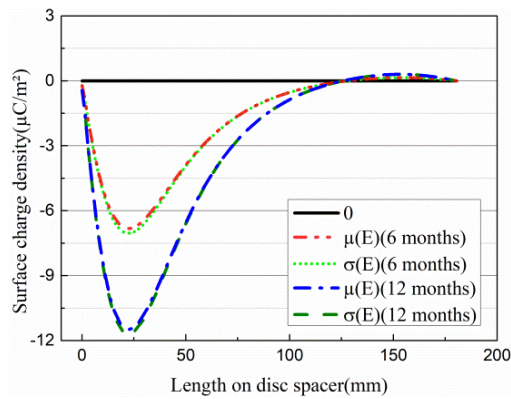


Figure 16. Surface charge density on the lower spacer boundary at +400 kV.

6 CONCLUSIONS

This paper studied the time-varying effect of surface charging phenomenon on spacers. A time-varying mathematical model is established, based on the influence of temperature and electric field on the ion mobility at the gas phase and the bulk conductivity in the solid phase. The principal findings are as follows:

(1) The normal component of the electric field strength of the spacer surface is closely related to the surface charge density. When the normal component of the electric field is negative, the surface area of the spacer is positively charged, and it is vice versa for positive electric field.

(2) When considering the influence of temperature on the conductivity of the solid, the surface charge density of the spacer can be increased very quickly. The maximum surface charge density on the spacer reaches 88.5 in 1 year, which is 5.85 times higher than that when the temperature is not considered.

(3) When the bulk conductivity is taken into account, the surface charge density of the spacer reaches about 13.3 $\mu\text{C}/\text{m}^2$ after 1 year, which is nearly 2.7 % higher compared with the case when the field strength was neglected. However, the change of the surface charge density of the spacer is minimal when considering the influence of the field intensity on the ion mobility.

ACKNOWLEDGMENT

This work was supported in part by the National Natural Science Foundation of China (Grant No. 51677113).

REFERENCES

- [1] C. Y. Li, C. J. Lin, W. D. Liu, J. Hu, B. Zhang, and J. L. He, "Novel HVDC spacers by adaptive control of surface charges – Part I: Charge transport and control strategy," *IEEE Trans. Dielectr. Electr. Insul.*, vol. 25, pp. 1238-1247, 2018.
- [2] C. M. Cooke, "Charging of insulator surfaces by ionization and transport in gases," *IEEE Trans. Dielectr. Electr. Insul.*, vol. EI-17, Issue 2, pp. 172-178, 1982.
- [3] A. Winter and J. Kindersberger, "Transient field distribution in gas-solid insulation systems under DC voltages," *IEEE Trans. Dielectr. Electr. Insul.*, vol. 21, pp. 116-128, 2014.
- [4] C. Zhang, X. Wang, Y. Zhou, Q. Xie, P. Yan, and T. Shao, "Electrical characteristics in surface dielectric barrier discharge driven by microsecond pulses," *IEEE Trans. Plasma Sci.*, vol. 44, pp. 2772-2778, 2016.
- [5] G. M. Ma, H. Y. Zhou, C. R. Li, J. Jiang, and X. W. Chen, "Designing Epoxy Insulators in SF₆-Filled DC-GIL with

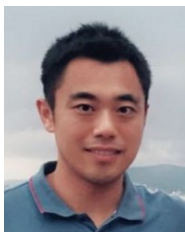
Simulations of Ionic Conduction and Surface Charging," *IEEE Trans. Dielectr. Electr. Insul.*, vol. 22, pp. 3312-3320, 2015.

- [6] C. Y. Li, C. J. Lin, B. Zhang, W. D. Liu, J. Hu, and J. L. He, "Understanding surface charge accumulation and surface flashover on spacers in compressed gas insulation," *IEEE Trans. Dielectr. Electr. Insul.*, vol. 25, pp. 1152-1166, 2018.
- [7] U. Straumann, M. Schüller, and C. M. Franck, "Theoretical investigation of HVDC disc spacer charging in SF₆ gas insulated systems," *IEEE Trans. Dielect. Electr. Insul.*, vol. 19, no. 6, pp. 2040-2048, 2011.
- [8] A. Winter, J. Kindersberger, M. Tenzer, and V. Hinrichsen, L. Zavattoni, O. Lesaint, M. Muhr, D. Imamovic, "Solid/gaseous insulation systems for compact HVDC solutions," presented at the Conference on CIGRE Session 45. Paris, France, 2014.
- [9] C. Y. Li, J. Hu, C. J. Lin, and J. L. He, "The neglected culprit of DC surface flashover- electron migration under temperature gradients," *Scientific Reports*, vol. 7, pp. 1-11, 2017.
- [10] Liu S, Zhou H, Ma G, et al. "Thermal field calculation in gas insulated busbars based on fluid multiple species transport," *Annu. Rep. Conf. Electr. Insul. Dielect. Phenom. (CEIDP)*, 2017, pp. 181-184.
- [11] R. Gremaud, F. Molitor, C. Doiron, T. Christen, U. Riechert, and U. Straumann, et al., "Solid insulation in DC gas-insulated systems," presented at the Conference on CIGRE Session 45. Paris, France, 2014.
- [12] R. Morrow, "A survey of the electron and ion transport properties of SF₆," *IEEE Trans. Plasma Sci.*, vol. 14, pp. 234-239, 1986.
- [13] B. Lutz and J. Kindersberger, "Surface charge accumulation on cylindrical polymeric model insulators in air: simulation and measurement," *IEEE Trans. Dielectr. Electr. Insul.*, vol. 18, pp. 2040-2048, 2011.
- [14] J. K. Kim, S. C. Hahn, K. Y. Park, H. K. Kim, and Y. H. Oh, "Temperature rise prediction of EHV GIS bus bar by coupled magneto thermal finite element method," *IEEE Trans. Dielectr. Electr. Insul.*, vol. 41, pp. 1636-1639, 2005.
- [15] T. Donen, H. Iwabuchi, S. Matsuoka, et al. "Influence of surface-conductivity non-uniformity on charge accumulation phenomena of GIS insulator under DC electric field," *IEEE Trans. Power and Energy*, vol. 131, pp. 584-590, 2011.
- [16] Lin, C., Li, C., He, J., Hu, J., and Zhang, B. "Surface charge inversion algorithm based on bilateral surface potential measurements of cone-type spacer," *IEEE Trans. Dielectr. Electr. Insul.*, vol. 24, pp. 1905-1912, 2017.



Wu Yan was born in JingZhou city, China, in 1993. He received the B.S. degree in physics from Huazhong University of Science and Technology Wen Hua College in 2015. Currently he is working for Master degree in electrical engineering at Shanghai University of Electric Power, Shanghai, China. His research interests is surface charge accumulation on high voltage insulator under dc.





Chuanyang Li was born in Shandong, China, on 6 February 1987. He received his double B.S. degrees of Electrical Engineering and English in Taiyuan University of Technology. After that, he spent 3 years to obtain his M.S. degree from the Department of Electrical Engineering, Taiyuan University of Technology, from 2011 to 2014. He received his Ph.D degree in the Department of Electrical Engineering, Tsinghua University in 2018.

Currently, he works as a Postdoctoral Fellow at the Department of Electrical, Electronic and Information Engineering “Guglielmo Marconi” of the University of Bologna (Alma Mater Studiorum - Università Di Bologna), Italy. His research interests include surface charge behavior, material modification for dielectrics in GIS/GIL, online monitoring for power cable insulation, and PD pattern recognition of HV motors and generators. He is the author and coauthor of more than 40 scientific papers. He can be reached by: lichuanyangsuper@163.com.

Zhipeng Lei was born in Taiyuan, China in 1983. He received the B.Sc. degree from the East China Jiaotong University, China in 2005, and the M.Sc.

degree, Ph.D. degree from the Taiyuan University of Technology, China in 2010 and 2015, respectively. He joined the College of Electrical and Power Engineering in the Taiyuan University of Technology as a lecturer since 2015. His main research interest is the condition assessment of high voltage cable failure and associated partial discharges characteristics, intelligence techniques in coal mine.

Tao Han (M'16) was born in Shandong, China. He received the M.E. and Ph.D. degrees in electrical engineering from Tianjin University, China, in 2012 and 2015, respectively. Since 2015, he has been a lecturer at School of Electrical Engineering and Automation in Tianjin University, China. His main research interests are degradation of cable insulation and partial discharge detection.



Zhousheng Zhang was born in Enshi city, China, in 1969. He received the B.S. degree in physics from Huazhong Normal University in 1992. He received the M.S. degree in electrical engineering from Huazhong University of Science and Technology in 1999. He received

the Ph.D. degree in electrical engineering from Shanghai Jiaotong University in 2010. Currently, he is a Professor with the Shanghai University of Electric Power. His current research interests include gas discharges, electrical insulation and materials, and condition monitoring of power apparatus. He can be reached by: zzsheng417@163.com.